

Effect of Three Chlorinated Ethenes on Growth Rates for a Methanotrophic Mixed Culture

JAMES E. ANDERSON* AND
PERRY L. MCCARTY

Department of Civil Engineering, Stanford University,
Stanford, California 94305-4020

The presence of chlorinated aliphatic hydrocarbons (CAHs) was found to decrease the net growth rate of a methanotrophic mixed culture expressing particulate methane monooxygenase (pMMO). Growth rates in the absence of CAHs were 1.48, 1.14, and 0.45 day⁻¹ on 460, 46, and 9.3 µg/L methane, respectively. Weighted nonlinear least squares fitting of the Monod model with decay yielded best estimates (±95% confidence intervals) of 2.67 ± 0.08 µg of methane (µg of cells)⁻¹ day⁻¹ for the maximum methane utilization rate, 15.6 ± 1.2 µg of methane/L for the methane half-saturation coefficient, and 0.20 ± 0.05 day⁻¹ for the endogenous respiration rate. Using this single set of kinetic parameter values, the model fit captured both the shape and the spacing of methane depletion curves covering 4 orders of magnitude in initial biomass concentration and 2 orders of magnitude in methane concentration. Growth rates on 460 µg/L methane were reduced by approximately 20% in the presence of 0.05 mg/L 1,1-dichloroethylene (1,1-DCE), 1 mg/L *trans*-1,2-dichloroethylene (t-DCE), or 1 mg/L trichloroethylene (TCE). A model for the effect of CAHs on growth rate was fitted to growth rate data by nonlinear least squares analysis. Competitive inhibition appeared the important factor for the reduction in growth rates with TCE and t-DCE, and transformation product toxicity was most significant for 1,1-DCE. Finally, an inoculum expressing sMMO showed an extreme toxicity in the presence of 0.005 mg/L 1,1-DCE, but not when the inoculum expressed pMMO.

Introduction

Trichloroethylene (TCE) was first shown to be aerobically biodegraded through the addition of natural gas containing methane to contaminated soil (1). Later studies demonstrated that methane, propane, ammonia, phenol, and toluene (2-5) oxidizing bacteria can oxidize many other chlorinated aliphatic hydrocarbons (CAHs) besides TCE

(4, 6). With methane-oxidizing (methanotrophic) bacteria, methane monooxygenase (MMO) catalyzes the oxidation of both CAH and the growth substrate, methane. Competitive inhibition by CAHs slows the rate of methane utilization (7) and vice versa (3, 8-12). Oxidation of both CAH and methane by MMO requires the input of reducing energy in the form of nicotinamide adenine dinucleotide (NADH) (13). Subsequent steps in the methane oxidation pathway regenerate the NADH consumed, but the CAH products provide no apparent benefit. Further methanotrophic oxidation of formate, one of many products of TCE transformation (14), may regenerate NADH, but MMO oxidation of other products (e.g., carbon monoxide) consumes additional NADH (10). Still other products are not oxidized by methanotrophs (15). Competitive inhibition of methane oxidation may exacerbate the situation by decreasing the rate of NADH regeneration. These processes singly or together may limit the rate of methane and CAH oxidation by MMO.

Organisms that oxidize CAHs experience toxic effects from the CAH transformation product or from further breakdown products (11, 16-19). Covalent binding of transformation products to a variety of cellular macromolecules has been observed (11, 14). Of importance for application of cometabolic processes for CAH degradation is the mass of CAH that can be transformed by a unit mass of cells, this is termed the transformation capacity (T_c , mg of CAH/mg of cells) (20). T_c quantifies the combined effects of several phenomena, relating the effect of transformation product toxicity (TPT). For a given culture, TPT varies greatly among different CAHs (21). Because of the complexity of possible TPT effects, the transformation capacity concept can be a useful engineering tool for engineering design purposes.

The kinetics of chlorinated ethene transformation by methanotrophs have been widely studied. However, few researchers have studied the effect of CAHs on methane utilization (9) and growth (7, 22) or have attempted to model this relationship (9, 23). Such information is of importance for the design of treatment systems where cell growth and CAH degradation occur simultaneously.

In the absence of CAHs, the net growth rate (μ , day⁻¹) of active organisms using the Monod relationship may be related to the rate of methane utilization:

$$\mu = \frac{1}{X_a} \frac{\partial X_a}{\partial t} = Y \left(\frac{k_s S}{S + K_s} \right) - b \quad (1)$$

where X_a is the active biomass concentration (µg/L), t is time (days), Y is biomass yield (µg of biomass/µg of cells), k_s is the methane maximum oxidation rate (µg of methane (µg of biomass)⁻¹ day⁻¹), K_s is the methane half-saturation concentration (µg/L), S is the methane concentration (µg/L), and b is the endogenous respiration rate (day⁻¹).

The presence of CAHs may reduce the growth rate of the organism by the processes discussed above. In an attempt to consider these process effects, eq 2 was formulated by Criddle (23), incorporated into a model of biofilm kinetics by Anderson and McCarty (24), and reported in a rearranged form by Chang and Alvarez-Cohen (9). The middle term on the right side reflects loss of active cells due to TPT and is quantified as the rate of CAH transfor-

* To whom correspondence should be addressed; telephone: 415-723-0315; fax: 415-725-3162.

mation divided by T_c . Competitive inhibition of methane utilization by the CAH is reflected in the modifier of K_s in the left term while inhibition of CAH transformation by methane (7) is represented by the K_c modifier in the middle term:

$$\mu = Y \left(\frac{k_s S}{S + K_s (1 + C/K_c)} \right) - \frac{1}{T_c} \left(\frac{k_c C}{C + K_c (1 + S/K_s)} \right) - b \quad (2)$$

where C is the CAH concentration (mg/L), K_c is the CAH half-saturation concentration (mg/L), and k_c is the CAH maximum oxidation rate (μg of CAH (μg of biomass) $^{-1}$ day $^{-1}$). Also, limitation in reducing energy availability (NADH) may decrease the oxidation rates of both methane and CAH (9, 23, 25) and may eventually stop these reactions altogether (9, 10, 26). As a result, eq 2 would not be valid by itself when reducing energy is rate limiting (9).

Growth rates are thus expected to be sensitive to changes in CAH as well as methane concentration. As methane concentration decreases or CAH concentration increases, the dual competitive inhibition terms both reduce μ . But CAH transformation would increase, thereby increasing the non-productive consumption of energy (NADH) as well as the production of toxic transformation products, all of which decrease growth rate.

The experiments described here were conducted with a culture expressing particulate MMO (pMMO). Whereas only some methanotrophs are capable of sMMO expression (under copper-limited conditions), all methanotrophs have the ability to express pMMO. Cultures expressing sMMO have received widespread study, because such cultures oxidize TCE at a much greater rate than pMMO-expressing cultures. However, typical conditions in nature are likely to favor pMMO expression (27, 28). Also, cultures expressing pMMO do rapidly oxidize some CAHs of importance, including *trans*-1,2-dichloroethylene (t-DCE) and vinyl chloride (VC) (6, 22, 26, 29).

Experimental Section

Chemicals. Methane (Liquid Carbonic Specialty Gas Co., San Carlos, CA) was of 99.0% purity. CAHs were added as saturated aqueous solutions (17), and included TCE (99+% pure ACS reagent, Aldrich Chemical Co., Milwaukee, WI), t-DCE (98% purity, Aldrich), and 1,1-dichloroethylene (1,1-DCE) (neat standard for EPA methods, Sigma Chemical Co., St. Louis, MO). Diluted 1,1-DCE stock solution was prepared by adding 37–370 μL of 1,1-DCE saturate to vials (4.7 mL) containing 2.0 mL of media and sealed with Teflon-lined silicone septa.

Mineral Medium and Sample Bottle Preparation. Mineral medium containing 0.074 μM copper was prepared with air-stripped deionized water using the formulation of Fogel et al. (30). Also included were 1.0 mg/L sodium thiosulfate and 1 mM sodium bicarbonate (31), the latter added after autoclaving and cooling.

Test tubes (15 mL) to be used for methane addition were weighed and inserted upside-down into 250-mL weighed glass serum bottles. After adding approximately 230 mL of mineral medium, the sealed bottles were autoclaved for 25 min at 121 $^{\circ}\text{C}$ and 2 atm pressure. The liquid volume was then adjusted so that 16.0 ± 0.1 mL headspace would remain after subsequent liquid additions.

Bacterial inoculum was added just before the start of an experiment. Controls received 220 mg/L sodium azide or no inoculum. Methane was added before sealing by means of a Pressure-Lok valved gas-tight syringe (Precision Sampling Co., Baton Rouge, LA) with a specially designed J-shaped needle to dispense methane up into the inverted 15-mL tube. CAH stock solution was injected just before sealing the bottle with an open-hole screw closure and both a Teflon-lined silicone septum and a Teflon-lined rubber septum. Each bottle was then briefly inverted in order to release the methane bubble into the headspace.

Inoculum Preparation. A methanotrophic mixed culture maintained in a continuous culture growth reactor (17) was used as the source of microorganisms. The dominant methanotrophic organism in this mixed culture has been isolated and shows 92% 16S rRNA homology to *Methylosinus trichosporium* OB3b (32), which expresses pMMO when sufficient copper is present (6, 33), but sMMO under the copper-limited conditions maintained in the growth reactor.

To ensure a consistent inoculum for the separate experiments, 1-mL aliquots of cells from the growth reactor were frozen in autoclaved 1.5-mL microcentrifuge tubes and stored for later use. Each tube received a total of 7.0 μL of dimethyl sulfoxide (DMSO), was vortexed lightly, and as subsequently suspended for 3 min in an ethanol and dry ice bath (approximately -77°C) for flash freezing, and then stored at -80°C .

Before an experiment, a culture tube was thawed at 0°C for 1 h, and then diluted into 200 mL of mineral medium. Bottles with 230 mL of mineral medium received 0.5 mL of this dilution and 0.5 mL of 99% methane and were incubated until more than 99.9% of the methane was removed. In these and all other experiments, bottles were incubated in the dark at 20°C with 150 rpm rotary shaking. Subsamples from the bottle were then used as inoculum for experiments. Under the above growth conditions, the organisms in the inoculum preparation bottle had a copper to biomass ratio of greater than 78 $\mu\text{mol/g}$ and reverted to pMMO expression as demonstrated by undetectable naphthalene oxidation (8). The copper to biomass concentration in experiments varied with growth time and due to differences in initial biomass and methane concentrations, but this ratio was never less than 78 $\mu\text{mol/g}$.

Inoculum Dilution Series. An inoculum dilution series experiment was used to determine the kinetic parameters in the absence of CAHs (eq 1) and resulting net growth rates at initial methane concentrations of 9.3, 46, and 460 μg of methane/L. Initial biomass concentrations spanning 4 orders of magnitude were evaluated at each methane concentration.

Weighted Nonlinear Least Squares Parameter Estimation. The results for all 44 bottles without CAHs were analyzed using a weighted NLS parameter estimation technique (34, 35) to determine k_s , K_s , b , and an additional parameter, $X_{0,\text{max}}$. Y was assumed to equal 0.64 μg of cells/ μg of methane (35). The rate of change of methane concentration in the liquid phase (S , $\mu\text{g/L}$) here is based on Monod kinetics corrected for gas/liquid mass transfer (35):

$$\frac{\partial S}{\partial t} = - \frac{k_s S}{S + K_s} X_a + K_L a \left(\frac{S_G}{H_c} - S \right) \quad (3)$$

where S_G is the headspace methane concentration ($\mu\text{g/L}$),

H_c is the dimensionless Henry's constant = 28.5 (–), and $K_L a$ is the mass transfer coefficient (day^{-1}). Likewise, headspace methane concentration seeks equilibrium with respect to the solution concentration:

$$\frac{\partial S_G}{\partial t} = -K_L a \frac{V_L}{V_G} \left(\frac{S_G}{H_c} - S \right) \quad (4)$$

where V_L is the liquid volume (L) and V_G is the gas volume (L).

Because of the complexity of the model (consisting of eqs 1, 3, and 4), a numerical solution was implemented. The FORTRAN code consisted of a fourth-order accurate Runge–Kutta scheme (36) run on a Sun SPARCstation 20. Initial conditions were the known methane concentrations after accounting for partitioning between liquid and headspace, and the initial active organism concentration, $X_0 = DX_{0,\text{max}}$, where D (–) is the inoculum dilution factor between the given bottle and that with the highest initial biomass ($X_{0,\text{max}}$, $\mu\text{g/L}$). Liquid and headspace volumes equaled 0.23 and 0.016 L, respectively. The mass transfer coefficient was determined experimentally by monitoring headspace methane after injection of a known volume of methane, from which $K_L a$ was found to equal $140 \pm 9 \text{ day}^{-1}$.

For every observation (methane concentration), the corresponding error was calculated as the difference between the actual and predicted headspace concentrations. Determination of errors required multiple simulation runs of the model, covering all combinations of inoculum and initial methane concentrations. Calculation of approximate 95% confidence intervals and correlation coefficients for the parameter estimates was performed similar to that described by others (34, 35).

Growth Rate Estimation. The results from the above inoculum dilution series as well as that described later with CAHs were also analyzed using only the spacing between methane removal curves. The curves of methane versus time were similar in shape for a given initial methane concentration, but were shifted laterally depending on the initial biomass concentration. The use of this analysis requires that the initial biomass concentration be much less than the methane concentration ($X_0 \ll Y\alpha S_0$). The dimensionless parameter, $\alpha = 1 + H_c V_G/V_L = 2.98$, was used to account for methane in the headspace. The time to 50% methane removal ($t_{50\%}$, day) for each bottle was used to quantify the spacing.

With the low starting biomass concentration, the growth rate μ remains essentially constant as long as $S \approx S_0$. However, this condition is no longer met after $t_{50\%}$ ($S = 1/2 S_0$). At this time, the biomass concentration equals $X_{50\%}$ (μg of biomass/L). X_0 was established using inoculum dilutions and thus was determined by the dilution factor, D . Rearranging the exponential growth equation

$$\frac{X_{50\%}}{X_0} = \frac{X_{50\%}}{DX_{0,\text{max}}} = e^{\mu t_{50\%}} \quad (5)$$

yields the following:

$$t_{50\%} = -\frac{1}{\mu} \ln(D) + \frac{1}{\mu} \ln(X_{50\%}) - \frac{1}{\mu} \ln(X_{0,\text{max}}) \quad (6)$$

Because the initial biomass was here small compared to $X_{50\%}$ ($X_0 \ll 1/2 Y\alpha S_0$), $X_{50\%}$ essentially represents the yield of organisms from the methane consumed and is thus a

constant for a given initial methane concentration ($X_{50\%} \approx 1/2 Y\alpha S_0$). $X_{0,\text{max}}$, also a constant, is the maximum inoculum concentration used in the dilution series. The growth rate μ was also essentially constant over this time period. Thus, the latter two terms in eq 6 represent a constant, C , so that there is a linear dependence of $t_{50\%}$ on $\ln(D)$:

$$t_{50\%} = -\frac{1}{\mu} \ln(D) + C \quad (7)$$

For each initial methane concentration, least squares linear regression of the measured $t_{50\%}$ values versus $\ln(D)$ yielded a slope equal to $-\mu^{-1}$. Confidence intervals (95%) for μ were estimated using the corresponding confidence intervals for the slope.

CAH Effect on Growth Rate. The variation of growth rate over a range of CAH concentrations was examined at 460 μg of methane/L and a single inoculum concentration (ca. 0.01 $\mu\text{g/L}$). For comparison, a separate set of bottles was inoculated with the same mixed culture (0.5 mL of a 0.1% dilution of the frozen cells), but initially expressed sMMO rather than pMMO. Controls received no inoculum and had mid-range CAH concentrations. Methane and CAH mass transfer rates between headspace and liquid were much greater than biological removal rates, so that gas/liquid equilibrium could be assumed.

The relationship between the time required for detectable methane removal and μ is similar to that for the inoculum dilution series, as appropriate test conditions were used, and is again based on eq 5, rearranged to give

$$\mu = \frac{1}{t_{50\%}} \ln \left(\frac{X_{50\%}}{X_0} \right) \quad (8)$$

In these experiments, X_0 was constant and $X_{50\%}$ was assumed to be independent of CAH concentration and thus also a constant. As a result, μ is inversely proportional to $t_{50\%}$. The value for μ determined without CAHs was used to estimate μ at different CAH concentrations based on

$$\frac{\mu_{\text{CAH}}}{\mu_{\text{noCAH}}} = \frac{t_{50\%,\text{noCAH}}}{t_{50\%,\text{CAH}}} \quad (9)$$

NLS error minimization was then used to estimate the CAH-related parameter values, with confidence intervals and correlation coefficients (35). This method for estimating the variation of μ with CAH concentration performed well, erring by less than 3% as determined by numerical solution of eq 2. Errors resulted because $X_{50\%}/X_0$ varied slightly at high CAH concentrations. As a result, eq 9 may not be applicable at higher CAH concentrations if that decreases $X_{50\%}$ by reducing cell yield.

Analytical Procedures. Methane was sampled (0.1 mL) from the headspace using a Precision Pressure-Lok gas-tight syringe and analyzed on a Hewlett-Packard 5730A gas chromatograph (GC) with a 5-ft Supelco 60/80 Carbosieve 1/8 in. diameter packed column at an oven temperature of 100 °C with a flame ionization detector. Using a dimensionless Henry's constant of 28.5 at 20 °C (37), one-third of the total methane mass was in solution and two-thirds was in the headspace.

CAH headspace samples (0.1 mL) were analyzed on a Tracor MT-220 GC with a 40–60 °C packed column containing 10% squalene on Chromosorb A/AW with a linearized electron capture detector. The column (J&W

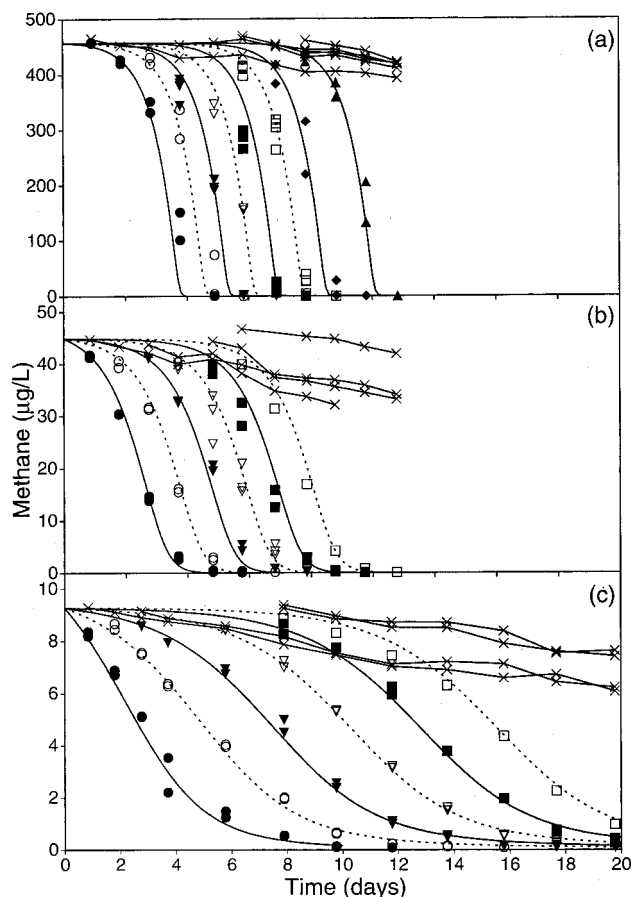


FIGURE 1. Methane concentration versus time for inoculum dilution series for three initial methane concentrations: (a) 460, (b) 46, and (c) 9.3 $\mu\text{g/L}$. Inoculum dilution factor: (●) 1, (○) 0.3, (▼) 0.1, (▽) 0.03, (■) 0.01, (□) 0.003, (◆) 0.001, (▲) 0.0001. Controls (×) had no inoculum added. Lines show corresponding model results using weighted NLS parameter estimates (Table 1).

Scientific) had a length of 30 m, an inner diameter of 0.53 mm, and a 3.0- μm DB-624 film and was used at 60 °C. Solution concentrations were calculated using dimensionless 20 °C Henry's constants of 0.299, 0.305, and 0.862 for TCE, t-DCE, and 1,1-DCE, respectively (38). CAHs partitioned primarily into the aqueous phase, with 94–98% of the total CAH mass in solution.

Results and Discussion

Inoculum Dilution Series. The inoculum dilution series results without CAHs present are illustrated in Figure 1. The pattern of methane removal with 460 μg of methane/L consisted of a variable time period with undetectable removal followed by a period of rapid removal (Figure 1a). Decreasing initial biomass concentrations increased the time prior to methane removal but had little effect on the shape of the curve. The curves for bottles containing lower methane concentrations (Figure 1b,c) were more sigmoidal in shape with a greater time interval between curves.

Weighted NLS Parameter Estimation. The Figure 1 results were used to estimate the kinetic parameter values describing methanotrophic growth (eq 1). The data were analyzed using both weighted and unweighted errors. The errors were more evenly distributed when weighted by the factor $w_i = 1/S_{\text{init},i}$ essentially normalizing the data by the initial methane concentration. With weighted errors, the distribution was 60%, 30%, and 10% among the 460, 46,

TABLE 1

Monod Parameter Value Best Estimates from Weighted NLS Fitting Using Inoculum Dilution Series Data without CAHs

parameter	best estimate ^a	correlation coefficient matrix ^b			
		k_s	K_s	b	$X_{0,\text{max}}$
k_s ($\mu\text{g } \mu\text{g}^{-1} \text{ day}^{-1}$)	2.67 ± 0.08	1			
K_s ($\mu\text{g/L}$)	15.6 ± 1.2	-0.94	1		
b (day^{-1})	0.20 ± 0.05	0.96	-0.96	1	
$X_{0,\text{max}}$ ($\mu\text{g/L}$)	3.69 ± 0.41	-0.82	0.75	-0.67	1

^a Best estimate and 95% confidence interval. ^b Correlation between parameter estimates.

and 9.3 $\mu\text{g/L}$ data. Even after this normalization, the high methane bottles still contributed the greatest error, most likely due to the steepness of the methane depletion curve (Figure 1a). Of the total 242 data points, five data points from the 460 $\mu\text{g/L}$ bottles were responsible for 36% of the error for the entire data set. The assumed value of the growth yield, Y , also did not greatly impact results. Increasing the value of Y resulted in a nearly proportional decrease in the value of k_s , while the other parameters were not affected. In short, the data were a good measure of the product of Y and k_s (μ_{max}), but not Y or k_s individually.

Abiotic losses of methane were neglected in model fitting. Losses did become significant many days after puncturing the septa in the initial sampling of no cell controls (Figure 1). However, active bottles were only punctured and sampled after the bottles having the next greater initial biomass concentration showed detectable (10%) methane removal. Thus, abiotic losses were minimal over the period when methane depletion was observed.

The best fit parameter values are reported in Table 1 with their approximate 95% confidence intervals and correlation coefficients. The results from model simulations using these parameter values are shown as curves in Figure 1, demonstrating that the Monod model with decay satisfactorily described the growth of this culture over a wide range of methane and inoculum concentrations. The confidence intervals for the estimates of k_s , K_s , and $X_{0,\text{max}}$ were narrow, indicating that the results were sensitive to these parameters. The low K_s value obtained is typical of pMMO under copper sufficient conditions, as expected, whereas values of 0.4–1.6 mg/L are typical for sMMO (28).

The estimates for k_s , K_s , and b were highly correlated (Table 1), implying that the data were not ideally suited for parameter estimation using this model. Confidence intervals about the parameter estimates would have been better had the correlation between parameters been less. The Figure 1 data was characterized by three distinct time periods: no methane removal at early times, an intermediate period of rapid removal, and an absence of methane at late times. Data were collected primarily with the intention of observing the onset of methane depletion, but not to sample frequently during this period. As a result, the data were actually a better indicator of growth rates, because such rates can be estimated by the time to 50% methane removal for different inoculum dilutions.

The negative correlation between k_s and K_s was unexpected. Typically, k_s and K_s are positively correlated, especially if the data are only taken at concentrations greater than K_s . However, when the sensitivity matrix neglected b and $X_{0,\text{max}}$, the correlation coefficient for k_s and K_s was

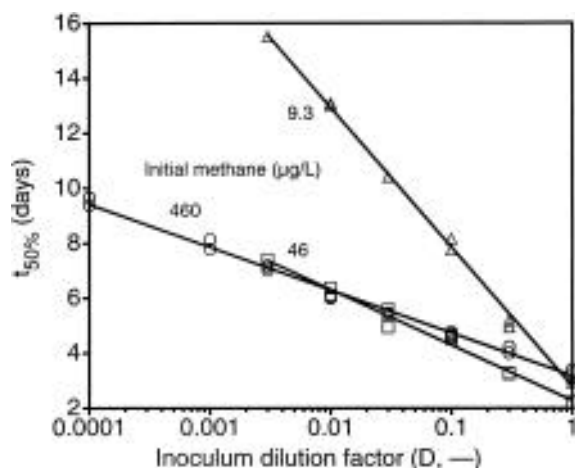


FIGURE 2. Effect of methane concentration on the time for 50% methane removal ($t_{50\%}$) versus inoculum dilution factor for the data in Figure 1. Three initial methane concentrations: (○) 460 $\mu\text{g/L}$, (□) 46 $\mu\text{g/L}$, (△) 9.3 $\mu\text{g/L}$. Lines show least squares log-linear fits.

TABLE 2

Growth Rates from Inoculum Dilution Series at Different Methane Concentrations and in the Presence of CAHs

CAH	concn (mg/L)	methane ($\mu\text{g/L}$)	growth rate ^a (day^{-1})	
			curve spacing ^b	NLS estimates ^c
none		9.3	0.45 (0.44–0.47)	0.44 (0.37–0.51)
none		46	1.14 (1.05–1.25)	1.07 (0.96–1.18)
none		460	1.48 (1.41–1.54)	1.46 (1.32–1.60)
TCE	1.0	460	1.07 (0.98–1.17)	<i>d</i>
t-DCE	4.7	460	0.68 (0.62–0.75)	<i>d</i>
1,1-DCE	0.0051	460	1.37 (1.28–1.47)	<i>d</i>

^a Growth rate and 95% confidence interval in parentheses. ^b Rates determined from linear regression of $t_{50\%}$ values versus natural logarithm of inoculum dilution factor using eq 7. ^c Rates calculated from eq 1 using NLS best fit parameter estimates in Table 1. ^d Not determined.

a positive 0.57. The negative correlation between k_s and K_s may be an artifact, resulting from the stronger positive correlation between k_s and b . An increase in k_s was best compensated by an increase in b , but a simultaneous decrease in K_s may have improved the overall fit.

Growth Rate Estimation. The NLS parameter estimation procedure indicated that the data set represented in Figure 1 was excellent for estimation of μ , but less so for the individual parameters because they were so closely correlated. Thus, the use of the $t_{50\%}$ method for directly estimating μ was felt appropriate. Using this approach, the growth rates obtained showed no dependence on inoculum concentration over the range examined, as demonstrated by the linearity of the data in Figure 2. Average growth rates at each of the three methane concentrations are reported in Table 2 with 95% confidence intervals. As expected for Monod kinetics (eq 1), μ increased with increasing methane concentration.

Whereas weighted NLS parameter estimation made use of all observations (3–9 per bottle), the curve spacing technique used only one value ($t_{50\%}$) for each bottle. These two approaches for estimating μ are compared in Table 2 for the case without CAHs present. Growth rates estimates by the two approaches were not significantly different at a 95% confidence level, providing validation for the simpler method of using $t_{50\%}$ values for growth rate determination.

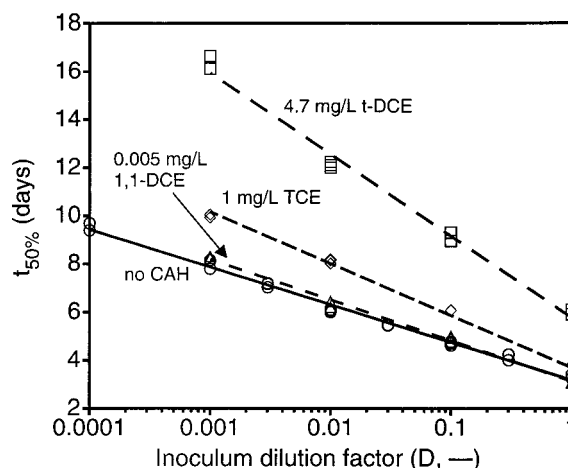


FIGURE 3. Effect of CAHs on the time for 50% methane removal ($t_{50\%}$) versus inoculum dilution factor: (○) no CAH, (△) 0.005 mg/L 1,1-DCE, (◇) 1 mg/L TCE, (□) 4.7 mg/L t-DCE. Lines show least squares log-linear fits.

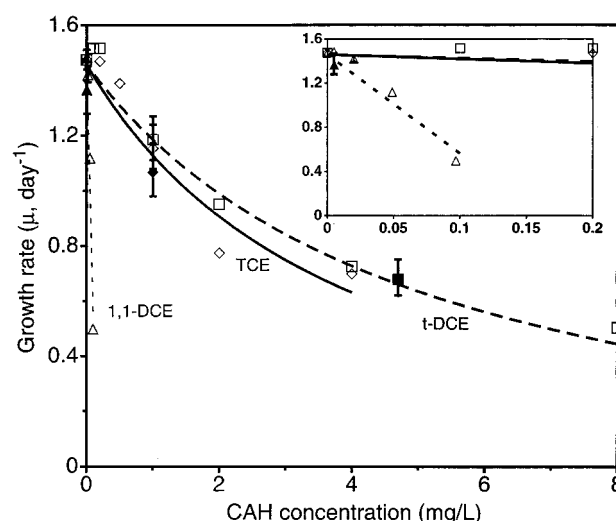


FIGURE 4. Growth rates versus CAH concentration determined from $t_{50\%}$ ratio analysis: (△) 1,1-DCE, (◇) TCE, (□) t-DCE. Initial methane concentration 460 $\mu\text{g/L}$. Triplicate bottles at 0.02 mg/L 1,1-DCE, 1 mg/L TCE, and t-DCE. Filled symbols indicate values from inoculum dilution series. Error bars indicate 95% confidence intervals. Lines show eq 2 model results using Table 1 and three-parameter values. For 1,1-DCE, the two- and one-parameter model results are indistinguishable. Inset shows lower CAH concentrations.

CAH Effect on Growth Rate. Three sets of inoculum dilutions series bottles were prepared with a mixture of a single concentration for each CAH and 460 μg of methane/L. Again, the $t_{50\%}$ values were linear with respect to $\ln(D)$ (Figure 3). The net growth rate was reduced by 28%, 54%, and 7% in the presence of 1 mg/L TCE, 4.7 mg/L t-DCE, and 0.005 mg/L 1,1-DCE, respectively (Table 2). The growth rate reductions with TCE and t-DCE, but not with 1,1-DCE at the low concentration used, were significant at a 95% confidence level.

A single small inoculum (0.01 $\mu\text{g/L}$) was used to observe the effect on growth rate from a range of CAH concentrations. Resulting growth rates are shown in Figure 4. Clearly, 1,1-DCE had the most adverse effect, causing a 24% and 66% reduction in μ at 0.05 and 0.10 mg/L 1,1-DCE, respectively. The presence of 1 mg/L TCE and 1 mg/L t-DCE reduced μ by 22 and 20%, respectively.

Single bottles were generally used for each CAH concentration, so little statistical information can be inferred.

TABLE 3

CAH-Related Parameter Best Estimates from NLS Fitting of Growth Rate Data with CAHs

CAH	k_c/T_c ^a (day ⁻¹)	K_c ^a (mg/L)	correlation coefficient	$k_c/T_c K_c$ (L mg ⁻¹ day ⁻¹)
TCE	0 ± 1.13	0.13 ± 0.15	0.978	0 ± 8.7
t-DCE	0 ± 0.44	0.17 ± 0.08	0.956	0 ± 2.6
1,1-DCE	115 ± 11000	0.43 ± 41	1.000	269 ± 37000
1,1-DCE ^c				262 ± 45

^a Best fit and approximate 95% confidence interval. ^b Correlation between parameter estimates. ^c Best fit and 95% confidence interval for estimate of $k_c/T_c K_c$ when $S/K_s \gg C/K_c$.

However, five replicates were run in the absence of CAHs and three each at 0.02 mg/L 1,1-DCE, 1 mg/L t-DCE, and 1 mg/L TCE. Replicates showed good agreement, with the $t_{50\%}$ values for each condition having coefficients of variation of less than 3%.

Both experiments for estimating growth rates showed roughly the same CAH dependence (Figure 4). Growth rates by inoculum dilution series and by $t_{50\%}$ ratio were not significantly different at the CAH concentrations where this could be determined. However, of the two methods, the inoculum dilution series can be expected to provide the most accurate growth rate estimates, although it requires more experimental effort.

NLS Parameter Estimation. Parameter estimates for the methane-related parameter values for the mathematical model describing the effect of CAHs on μ (eq 2) are summarized in Table 1. To consider the effect of CAHs, two additional parameter values are required: k_c/T_c and K_c . The ratio k_c/T_c (day⁻¹) represents the maximum specific rate of active biomass loss due to transformation product toxicity. Growth rates as a function of CAH concentrations were used to determine k_c/T_c and K_c using NLS fitting with eq 2. Resulting values, confidence intervals, and correlation coefficients are reported in Table 3. Resulting model fits are shown in Figure 4.

For both TCE and t-DCE, the best fits obtained were with $k_c/T_c = 0$, but the confidence intervals were broad. Results from a separate study specifically designed to measure CAH transformation rates and capacities for this culture indicated that, for TCE, T_c was 0.025 mg of TCE/mg of cells (26) and k_c was at least 0.012 mg of TCE (mg of cells)⁻¹ day⁻¹, giving a k_c/T_c value of 0.48 day⁻¹. This value lies within the confidence interval for the value estimated by NLS (0 ± 1.13 day⁻¹, Table 3). For t-DCE, T_c was 3.4 mg of t-DCE/mg of cells and k_c was at least 4.2 mg mg⁻¹ d⁻¹ (39), giving a k_c/T_c of 1.2 day⁻¹, which is outside the confidence interval bounds in Table 3.

The uncertainties in the exact values of k_c/T_c for TCE and t-DCE make statements more speculative about the relative influences of competitive inhibition and transformation product toxicity on growth rate reduction as represented in eq 2. If k_c/T_c were zero, then this reduction would all be due to competitive inhibition. However, even with the alternative values given above, 80% and 60% of the growth rate reduction by TCE and t-DCE, respectively, would be due to competitive inhibition. Thus, for these two CAHs, competitive inhibition is certainly the dominant, if not the sole factor causing the observed growth rate reductions.

On the other hand, for 1,1-DCE, the parameter estimates (Table 3) indicate that 99% of the reduction in μ was due

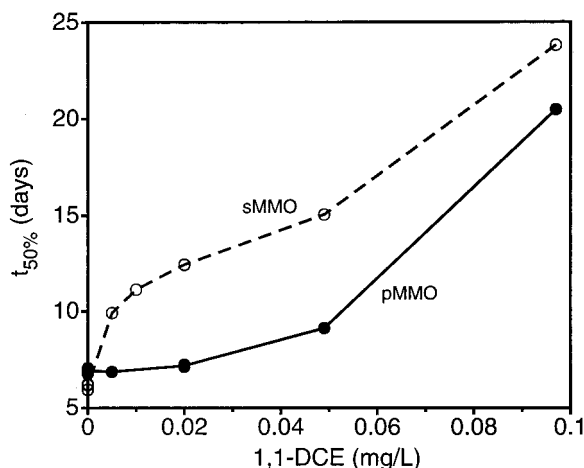


FIGURE 5. Effect of initial MMO type, (●) pMMO or (○) sMMO on the time for 50% methane removal ($t_{50\%}$) versus 1,1-DCE concentration. Cultures initially expressing sMMO reverted to pMMO after an undetermined time. Lines show average $t_{50\%}$ values. Five bottles used at 0 mg/L 1,1-DCE and three at 0.02 mg/L 1,1-DCE.

to TPT. The perfect correlation between k_c/T_c and K_c suggest that the ratio of the two parameters ($k_c/T_c K_c$) is a more appropriate representation of the effect of 1,1-DCE on μ . When $S/K_s \gg C/K_c$, as was here the case for 1,1-DCE, eq 2 can be simplified so that the parameter ratio can be used directly:

$$\mu = Y \left(\frac{k_s S}{S + K_s} \right) - \frac{k_c}{T_c K_c} \left(\frac{C}{S/K_s} \right) - b \quad (10)$$

With this equation, the effect of CAHs on μ is exclusively due to TPT. NLS fitting for the combined parameter ratio ($k_c/T_c K_c$) resulted in a much narrower confidence interval (Table 3). The fit for the 1,1-DCE data using eq 10 is indistinguishable from that using eq 2 (Figure 4). If K_c for 1,1-DCE was 0.17 mg/L, the same as that for t-DCE, then k_c/T_c would be 45 day⁻¹, nearly 2 orders of magnitude greater than for TCE or t-DCE.

Effect of MMO Type Initially Expressed by Inoculum.

A separate set of bottles inoculated with the same mixed culture expressing sMMO was run concurrent with bottles containing pMMO inoculum. The time to 50% methane utilization ($t_{50\%}$) is plotted versus 1,1-DCE concentration in Figure 5. The addition of 1,1-DCE at a concentration as low as 0.005 mg/L caused $t_{50\%}$ to increase significantly with sMMO expression, but had little or no effect with pMMO expression. The copper to biomass ratio of this experiment was such that the sMMO inoculum would switch to pMMO expression during the experiment. Others (26, 35) have found such a transition to require 2–10 h. During this time, the inoculum would have a higher 1,1-DCE transformation rate, as 1,1-DCE and TCE transformation rates are typically orders of magnitude greater for sMMO than pMMO (6, 21, 27). Thus, while the inoculum expressed sMMO, the cells would experience much greater TPT from 1,1-DCE transformation. Methane utilization and growth were eventually observed in these bottles, indicating that μ then reverted to a positive value. The increase in the time to methane removal ($t_{50\%}$) indicates the time required for the inoculum to recover from TPT losses. This apparent sMMO-enhanced toxicity was also observed with TCE and t-DCE, but to a much lesser extent, most likely because TPT from 1,1-DCE cometabolism is an order of magnitude more severe than from TCE or t-DCE (21).

Summary and Implications. The experiments described here were conducted with a mixed culture, as would typically be found under in-situ field conditions or in large-scale aboveground systems. Spacing between methane depletion curves for bottles having different initial biomass concentrations were used to estimate growth rates. Ideally, directly enumeration of active biomass would be used to corroborate the presumed increase in active biomass with growth, as has been shown by others (40). However, such methods were inappropriate here as they typically fail to discriminate between cells that are active or inactive toward methane and CAHs (26). Low biomass concentrations made other techniques infeasible. The method described here is an activity-based technique that worked well for a methanotrophic mixed culture. The strong correlation between the time to 50% methane removal and active cell population supports the use of this measure for the enumeration of active populations within a mixture (26).

The presence of each CAH was found to reduce the net growth rate of the methane-oxidizing mixed culture. The effect on μ appears to depend on the affinity of the MMO enzyme for the CAH (K_c), as well as the rate of CAH transformation (k_c) and the resulting energetic requirement and toxicity of transformation products (T_c). Based on the K_c values determined through NLS fitting, TCE and t-DCE reduce μ primarily through competitive inhibition of methane utilization at the methane concentration used in this study. (At lower methane concentrations, TPT is expected to be of more importance as compared to competitive inhibition.) The TPT from TCE oxidation was less significant because the rate of TCE transformation was low. Likewise, the faster rate of t-DCE oxidation was offset by a larger T_c . On the other hand, 1,1-DCE concentrations were too low to competitively inhibit methane utilization, yet this CAH had the greatest impact on μ . Even though the rate of 1,1-DCE transformation was too low to be determined accurately, the associated TPT was extreme. Even greater toxicity from 1,1-DCE was observed when the culture initially expressed sMMO, most likely due to a higher rate of CAH transformation compared to that with pMMO. In either case, the concentration of 1,1-DCE transformation products is likely to be very low. The extreme toxicity observed suggests a potent mechanism for cellular inactivation, such as covalent binding within the active site of sMMO. The exact mechanism of this important adverse effect deserves study.

Organisms expressing other oxygenases, such as toluene monooxygenase, may likewise be susceptible to 1,1-DCE. For example, in a pilot study of *in-situ* phenol addition to contaminated groundwater, TCE degradation was halved when 0.065 mg/L 1,1-DCE was supplemented into the injected groundwater (41). Conceivably, the presence of 1,1-DCE could virtually eliminate an *in-situ* population of oxygenase-producing organisms. A possible means for overcoming this limitation is to first grow a large population of appropriate organisms by providing an organism-specific growth substrate that does not induce oxygenase enzyme expression followed by an inducing substrate that would initiate CAH degradation by the grown population.

Acknowledgments

This material is based on work supported in part under a National Science Foundation Graduate Fellowship, in part under a Stanford/NIH Biotechnology Training Grant fel-

lowship, and in part by the Office of Research and Development, U.S. Environmental Protection Agency, through the Western Region Hazardous Substance Research Center, under Agreement R-815738. The contents of this paper do not necessarily represent the views of these agencies.

Literature Cited

- (1) Wilson, J. T.; Wilson, B. H. *Appl. Environ. Microbiol.* **1985**, *49*, 242–243.
- (2) Hopkins, G. D.; Semprini, L.; McCarty, P. L. *Appl. Environ. Microbiol.* **1993**, *59*, 2277–2285.
- (3) Chang, H.-L.; Alvarez-Cohen, L. *Biotechnol. Bioeng.* **1995**, *45*, 440–449.
- (4) Wackett, L. P.; Brusseau, G. A.; Householder, S. R.; Hanson, R. S. *Appl. Environ. Microbiol.* **1989**, *55*, 2960–2964.
- (5) Hyman, M. R.; Russell, S. A.; Ely, R. L.; Williamson, K. J.; Arp, D. J. *Appl. Environ. Microbiol.* **1995**, *61*, 1480–1487.
- (6) Oldenhuis, R.; Vink, R. L. J. M.; Janssen, D. B.; Witholt, B. *Appl. Environ. Microbiol.* **1989**, *55*, 2819–2826.
- (7) Broholm, K.; Christensen, T. H.; Jensen, B. K. *Water Res.* **1992**, *26*, 1177–1185.
- (8) Brusseau, G. A.; Tsien, H.-C.; Hanson, R. S.; Wackett, L. P. *Biodegradation* **1991**, *1*, 19–30.
- (9) Chang, H.-L.; Alvarez-Cohen, L. *Environ. Sci. Technol.* **1995**, *29*, 2357–2367.
- (10) Henry, S. M.; Grbic-Galic, D. *Appl. Environ. Microbiol.* **1991**, *57*, 1770–1776.
- (11) Oldenhuis, R.; Oedzes, J. Y.; van der Waarde, J. J.; Janssen, D. B. *Appl. Environ. Microbiol.* **1991**, *57*, 7–14.
- (12) Speitel, G. E., Jr.; Thompson, R. C.; Weissman, D. *Water Res.* **1993**, *27*, 15–24.
- (13) Dalton, H.; Stirling, D. I. *Philos. Trans. R. Soc. London B* **1982**, *297*, 481–496.
- (14) Fox, B. G.; Borneman, J. G.; Wackett, L. P.; Lipscomb, J. D. *Biochemistry* **1990**, *29*, 6419–6427.
- (15) Uchiyama, H.; Nakajima, T.; Yagi, O.; Nakahara, T. *Appl. Environ. Microbiol.* **1992**, *58*, 3067–3071.
- (16) Janssen, D. B.; Scheper, A.; Dijkhuizen, L.; Witholt, B. *Appl. Environ. Microbiol.* **1985**, *49*, 673–677.
- (17) Alvarez-Cohen, L. M.; McCarty, P. L. *Appl. Environ. Microbiol.* **1991**, *57*, 228–235.
- (18) Henry, S. M.; Grbic-Galic, D. *Microb. Ecol.* **1990**, *20*, 151–169.
- (19) Wackett, L. P.; Householder, S. R. *Appl. Environ. Microbiol.* **1989**, *55*, 2723–2725.
- (20) Alvarez-Cohen, L. M.; McCarty, P. L. *Environ. Sci. Technol.* **1991**, *25*, 1381–1387.
- (21) Dolan, M. E.; McCarty, P. L. *Environ. Sci. Technol.* **1995**, *29*, 2741.
- (22) Dolan, M. E.; McCarty, P. L. *Environ. Sci. Technol.* **1995**, *29*, 1892–1897.
- (23) Criddle, C. S. *Biotechnol. Bioeng.* **1993**, *41*, 1048–1056.
- (24) Anderson, J. E.; McCarty, P. L. *J. Environ. Eng.* **1994**, *120*, 379–400.
- (25) Bae, W.; Rittmann, B. E. *Biotechnol. Bioeng.* **1996**, *49*, 683–689.
- (26) Anderson, J. E. Ph.D. Thesis, Stanford University, 1996.
- (27) DiSpirito, A. A.; Gullledge, J.; Shiemke, A. K.; Murrell, J. C.; Lidstrom, M. E.; Krema, C. L. *Biodegradation* **1992**, *2*, 151–164.
- (28) Lidstrom, M. E.; Semrau, J. D. In *Aquatic Chemistry: Interfacial and Interspecies Processes*, 244th ed.; Huang, C. P., O'Melia, C. R., Morgan, J. J., Eds.; American Chemical Society: Washington, DC, 1995; pp 195–201.
- (29) Janssen, D. B.; Grobbsen, G.; Hoekstra, R.; Oldenhuis, R.; Witholt, B. *Appl. Microbiol. Biotechnol.* **1988**, *29*, 392–399.
- (30) Fogel, M. M.; Taddeo, A. R.; Fogel, S. *Appl. Environ. Microbiol.* **1986**, *51*, 720–724.
- (31) Park, S.; Hanna, M. L.; Taylor, R. T.; Drooge, M. W. *Biotechnol. Bioeng.* **1991**, *38*, 423–433.
- (32) Alvarez-Cohen, L.; McCarty, P. L.; Boulygina, E.; Hanson, R. S.; Brusseau, G. A.; Tsien, H. C. *Appl. Environ. Microbiol.* **1992**, *58*, 1886–1893.
- (33) Tsien, H.-C.; Brusseau, G. A.; Hanson, R. S.; Wackett, L. P. *Appl. Environ. Microbiol.* **1989**, *55*, 3155–3161.
- (34) Robinson, J. A. In *Advances in Microbial Ecology*; Marshall, K. C., Ed.; Plenum: New York, NY, 1985; Vol. 8, pp 61–114.
- (35) Smith, L. H.; Kitanidis, P. K.; McCarty, P. L. *Biotechnol. Bioeng.*, in press.
- (36) Press, W. H.; Flannery, B. P.; Teukolsky, S. A.; Vetterling, W. T. *Numerical Recipes. The Art of Scientific Computing (FORTRAN Version)*; Cambridge University: Cambridge, 1989.

- (37) *Perry's Chemical Engineers' Handbook*, 6th ed.; Perry, R. H., Green, D. W., Eds.; McGraw-Hill: New York, 1984.
- (38) Gossett, J. M. *Environ. Sci. Technol.* **1987**, *21*, 202–208.
- (39) Nielsen, A. K.; Gerdes, K.; Degn, H.; Murrell, J. C. *Microbiology* **1996**, *142*, 1289–1296.
- (40) Comeau, Y.; Greer, C. W.; Samson, R. *Appl. Microbiol. Biotechnol.* **1993**, *38*, 681–687.
- (41) Hopkins, G. D.; McCarty, P. L. *Environ. Sci. Technol.* **1995**, *29*, 1628–1637.

Received for review February 28, 1996. Revised manuscript received July 17, 1996. Accepted July 19, 1996.[®]

ES960187N

[®] Abstract published in *Advance ACS Abstracts*, October 1, 1996.